Springer

KSME

Journal of Mechanical Science and Technology 24 (11) (2010) 2289~2295
www.springerlink.com/content/1738-494x
DOI 10.1007/s12206-010-0901-7

# Analytical model for predicting the surface profile of a work piece in round-to-2–R and square-to-2–R oval groove rolling †

U. K. Yoo[1], J. B. Lee[2], J. H. Park[3] and Y. Lee[1,*]

[1]*Department of Mechanical Engineering, Chung-Ang University, Seoul, 156-756, Korea*
[2]*Rolling Technology & Process Control Group, POSCO Technical Research Laboratories, Pohang, 790-785, Korea*
[3]*Department of Computer Science, Chung-Ang University, Seoul, 156-756, Korea*

(Manuscript Received June 14, 2010; Revised August 10, 2010; Accepted August 24, 2010)

**Abstract**

This paper presents an analytical model that predicts the surface profile of a workpiece in a round-to-2–R oval groove and a square section-to-2–R oval groove rolling sequence. "2–R oval" indicates a profile of the roll groove that has two different radii of curvature. Using low carbon steel (S10C) and stainless steel (STS304), we conduct a hot groove rolling experiment to verify the robustness of the proposed model. Results show that the predicted surface profile and exit cross-sectional area are in good agreement with experimental results. The second radius of curvature of the 2–R oval groove is important in reducing the exit cross-sectional area of the workpiece and partly squeezing the workpiece outward (i.e., in the roll gap direction) when in contact with the workpiece. Therefore, the surface profile of the workpiece in the 2–R oval groove is smaller than that of the 1–R oval groove.

*Keywords*: Modeling; 2-R oval groove; Surface profile; Groove rolling

## 1. Introduction

In continuous hot rod (or bar) rolling, a billet is processed into the desired shape with acceptable dimensional tolerances as it passes through many stands. Here, "stand" denotes a unit machine that has work rolls with a certain groove shape, such as a box, oval, round, square, and diamond. To transform the billet into the desired final section, a pair of grooves, such as oval-to-square, oval-to-round (or vice versa), square-to-diamond (or vice versa), and diamond-to-diamond is placed repetitively in the rolling line; the magnitude of shapes diminishes with the size of the workpiece cross-section.

Among these groove shapes, the oval groove has various derivatives because its shape depends considerably on the radius of curvature. For example, the "2–R oval groove" indicates an oval groove with two radii of curvature. 1–R and 3–R oval grooves denote oval grooves that have one and three radii of curvature, respectively. The number of radii curvatures is determined by roll pass designers and the characteristics of the product. The wire rod mill in POSCO, in which carbon steels are mainly produced, uses the 1–R oval groove. The rod and bar mill in POSCO Specialty Steel, in which stainless and alloy steels are mainly produced, uses the 2–R oval groove. The bar mill in SEAH Specialty Steel in Korea, in which high alloy steels are generally manufactured, makes use of the 3–R oval groove.

To reduce inhomogeneous metal flow at the corner of the roll groove, decrease roll wear, and inhibit the generation of crack-like defects on the workpiece surface, designers should opt for the 1–R oval groove [1]. Using 2–R or 3–R oval grooves is preferred when a temperature drop at the edge of the workpiece cross-section must be minimized while the workpiece transfers from one stand to the next. In addition, 2–R and 3–R oval grooves increase the reduction ratio in a given pass (stand) because the spread of the workpiece inside the groove is restricted by the second or third radius of curvature.

Quickly calculating the surface profile of the outgoing workpiece at each pass and computing the "mass balance" between passes have always been challenging for roll pass designers. This "mass balance" is expressed as the product of the cross-sectional area of the outgoing workpiece and the roll speed at each pass. Finite element analysis is a very effective way to determine this, but this method consumes at least half an hour for a single pass [2–6]. A rod (or bar) rolling mill has a large number of passes (12 to 29 passes, for example); thus, a non-iteration-based analytical model that can rapidly compute the surface profile of an outgoing workpiece is highly desired.

† This paper was recommended for publication in revised form by Associate Editor Dae-Eun Kim
*Corresponding author. Tel.: +82 2 824 5256, Fax: +82 2 814 9476
E-mail address: ysl@cau.ac.kr

Lee and Choi [7] proposed an analytical model for predicting the surface profile of a workpiece in 1–R oval and round groove rolling. The advantage of this model is that the surface profile of the outgoing work piece at a pass is predicted using the cross-sectional geometry of the incoming workpiece, the geometry of the roll groove, and a weighting function that satisfies the constraint conditions of the rolling process. Lee [8] applied this model to the POSCO No. 3 Rod Mill, which has a 1–R oval groove and round groove rolling sequence, and demonstrated its usefulness.

In this study, the capability of the analytical model [7] is extended to predict the surface profile of the outgoing workpiece when a 2–R oval groove is employed. The design parameters of the 2–R oval groove are first described, and then the equations that interrelate these design parameters are derived. We then design a billet (square)-to-2–R oval groove and a round-to-2–R oval groove (or vice versa) rolling sequence. We conduct a pilot rolling test and illustrate the value of the proposed model by comparing measurement results to model predictions.

## 2. Design parameters in 2–R oval groove

Fig. 1 shows the front view of the 1–R oval and 2–R oval groove. Design parameters H and D indicate groove height and groove depth, respectively. The center of the larger radius of curvature, $R_1$, is positioned beyond the roll groove shape but along the y-axis. The center of the smaller radius of curvature, $R_2$, may be located inside the roll groove shape but need not be located along the *x*-axis. In Fig. 1(a), $FW_1$ represents the face width (FW) of the 2–R oval groove. In Fig. 1(b), $FW_2$ represents the distance between the points where a circle with radius of curvature $R_1$ and a line that has an angle $\alpha$ with respect to the y-axis meet [this point is not depicted explicitly in Fig. 1(b)]. The H and D of the 1–R and 2–R oval grooves are identical but their face widths are different. The 2–R oval groove is viewed such that the FW of the 1-R oval groove narrows because of the second radius of curvature $R_2$.

After the geometric relationship among the two radii of curvature, H, FW, and D of the 2–R roll groove is examined, the equation for the center point of $R_2$ ($X_2$, $Y_2$) is obtained as follows:

$$X_2 = \frac{b - \sqrt{b^2 - ac}}{a} \tag{1}$$

$$Y_2 = D - R_1 + \sqrt{(R_1 - R_2)^2 - X_1^2} \tag{2}$$

where

$$a = 1 + \tan^2 \alpha, \quad b = L \tan \alpha, \quad c = L^2 - (R_1 - R_2)^2 \tag{3}$$

Angle $\alpha$ and parameter L used in Eq. (3) are expressed as follows:

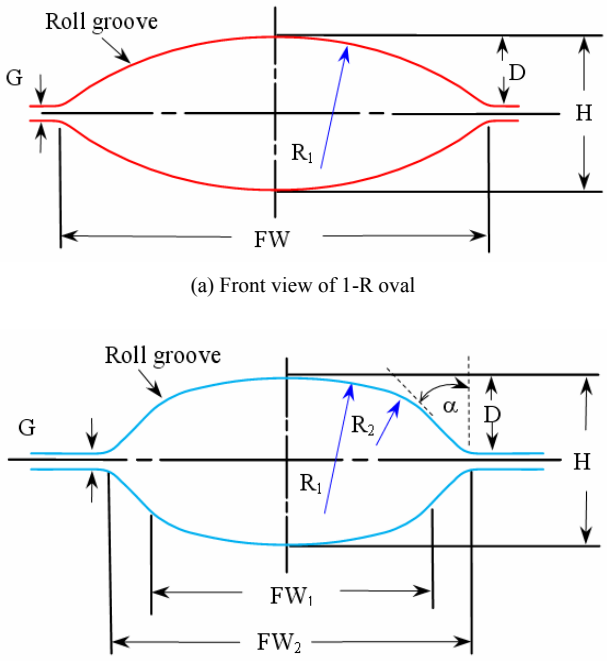


(a) Front view of 1-R oval

(b) Front view of 2–R oval

Fig. 1. Schematic of 1-R and 2–R oval grooves.

$$\alpha = \tan^{-1}\left( \frac{D - R_1 + \sqrt{R_1^2 - (FW_1/2)^2}}{\frac{FW_2}{2} - \frac{FW_1}{2}} \right) \tag{4}$$

$$L = \frac{FW_2}{2} \tan \alpha - \frac{R_2}{\cos \alpha} - D + R_1 \tag{5}$$

Therefore, once the design parameters D, H, $FW_2$, $FW_1$, $R_1$, and $R_2$ are determined, the center point of $R_2$ ($X_2$, $Y_2$) can be computed using Eqs. (1)-(5), and the 2–R oval groove shape can be drawn. Note that if the center of the smaller radius of curvature $R_2$ is on the *x*-axis, it is called a regular 2–R oval groove. A procedure for deriving the design parameters is explained in [9].

## 3. Prediction of the surface profile of the outgoing workpiece

To predict the surface profile of the outgoing workpiece at a pass, we must first determine its maximum spread. The surface profile of an outgoing workpiece is then computed based on the dimensions of the inlet cross-section of the workpiece and a weighting function linked with the geometry of the roll groove.

### *3.1 Maximum spread in groove rolling*

Shinokura and Takai [10] carried out experiments using a pilot rolling mill; using the wide range of experimental data as a basis, they developed a model to calculate the maximum spread for mild steel (JIS SS41) in four types of rolling se-

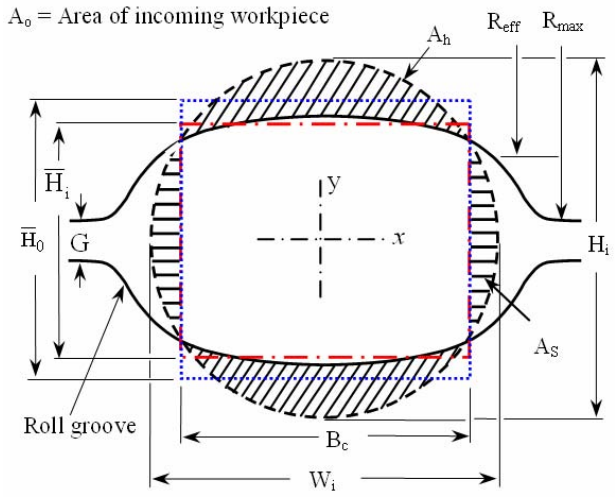


Fig. 2. Application of equivalent rectangle approximation into the round groove-to-2−R oval groove rolling sequence to calculate the effective height for the workpiece and the area fraction between the incoming workpiece and the geometry of the roll groove.

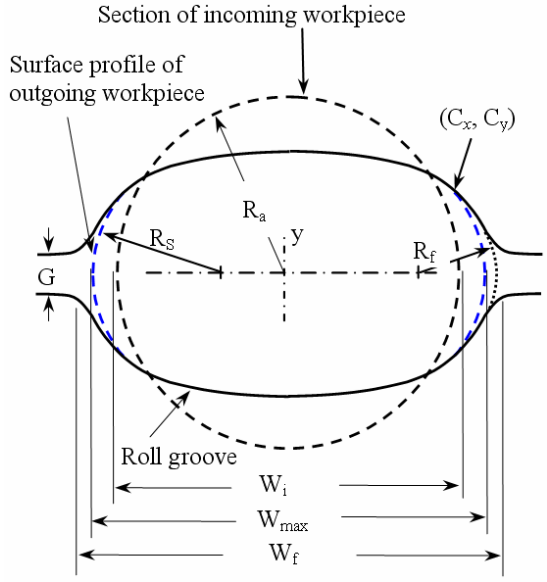


Fig. 3. Geometrical designation of the 2−R roll groove, the incoming workpiece, and the radius of the surface profile, $R_S$, of the outgoing workpiece in the round groove-to-2−R oval groove rolling sequence.

quences, namely, square-to-oval, round-to-oval, square-to-diamond, and diamond-to-diamond grooves. Their idea is that the maximum spread of an outgoing (exit) workpiece can be expressed as a function of roll radius, the geometry of an incoming (inlet) workpiece, and the area fraction between the incoming workpiece and the geometry of the roll groove.

Fig. 2 illustrates the application of the Shinokura and Takai model to a round-to-2–R oval groove rolling sequence. The maximum spread, $W_{max}$, was calculated using the following formula:

$$W_{max} = W_i\left[1+\gamma\frac{\sqrt{R_{mean}(\bar{H}_i-\bar{H}_o)}}{W_i+0.5H_i}\cdot\frac{A_h}{A_o}\right] \quad (6)$$

where

$$\bar{H}_o = \frac{A_o - A_s - A_h}{B_c};\ \bar{H}_i = \frac{A_o - A_s}{B_c}. \quad (7)$$

$W_i$ and $H_i$ are the maximum width and the maximum height of an incoming workpiece (i.e., the inlet cross-section), respectively, and γ stands for a spread correction coefficient that depends on the type of rolling sequence and material. This procedure can also be applied to 2–R oval-to-round or square-to-2–R oval groove rolling.

### *3.2 Surface profile of the outgoing workpiece in round-to-2–R oval groove rolling*

The geometric designation of the round-to-2–R oval groove rolling sequence is described in Fig. 3. $R_a$ is the radius of curvature of the inlet cross-section, $R_s$ represents the predicted radius of curvature of the outlet cross-section, and $R_1$ denotes the radius of the roll groove. When the incoming round workpiece is deformed at the inside of the oval groove and reaches the face width of oval groove $W_f$, the final surface profile of the deformed workpiece is assumed to be a circle of radius $R_f$. $R_f$ is approximated as the radius of a circle located within the roll groove area and passing through the point ($x = \pm W_f/2$, $y = 0$). Assuming that $W_{max}$ does not exceed $W_f$ (width of the roll groove area), $R_s$ is given by:

$$R_s = R_a \cdot W_t + R_f \cdot (1 - W_t), \quad (8)$$

where

$$W_t = \frac{W_f - W_{max}}{W_f - W_i}. \quad (9)$$

$W_t$ is a weighting function, $W_i$ is the width of the inlet cross-section, and $W_{max}$ denotes the maximum spread of the exit cross-section [which can be calculated using Eq. (6)]. $R_f$ is the radius to be achieved when $W_{max}=W_f$. An experiment need not be performed to determine the weighting function. The requirements for choosing the weighting function stem from the need to guarantee the relationship described by Eq. (8). According to Eqs. (8) and (9), $R_s$ becomes $R_a$ when $W_{max}=W_i$ (no spread), and $R_s$ becomes $R_f$ when $W_{max}=W_f$. $R_f$ denotes the radius of the workpiece surface profile when the maximum spread reaches $FW_1$. The ability to express $R_f$ in Eq. (8) in terms of the design parameter of the 2–R oval groove in a fully analytic manner is quite limited. Hence, in this study, it was approximated in a simple form as follows:

$$R_f = R_2 / 2 \quad (10)$$

Once $R_s$ is determined, the separating point ($C_x$, $C_y$) can be obtained and the area of the exit cross-section can be calculated. This route can also be applied to the 2–R oval-to-round groove rolling sequence.

### *3.3 Surface profile of the outgoing workpiece in square-to-2–R oval groove rolling*

In deriving Eqs. (8) and (9), no restrictions are placed on the shape of the inlet section of the workpiece. As a result, the equations can be applied to any shape of inlet section, such as a square, oval, or diamond. Hence, the modeling technique employed in Section 3.2 can easily be applied to an initial billet (square)-to-2-R oval groove rolling sequence. In this case, the radius of curvature of the inlet cross-section of the billet becomes infinite. In the proposed model, we assumed that the radius of curvature is twice the width (or height) of the billet.

## 4. Experiment

### *4.1 Rolling mill*

A single stand two-high laboratory mill was employed, driven by a 75 kW constant torque direct current motor. Ductile casting iron rolls with a 310 mm diameter and 320 mm face width were used. The rolling speed was set at about 0.5 m/s.

### *4.2 Specimen and roll groove design*

Low carbon steel and stainless steel were used. The materials were obtained in the form of square as-cast billets with a side length of 160 mm. The specimens to be rolled were cut and machined into round bar specimens of 60 mm diameter and 300 mm length for the round-to-2–R oval groove rolling test. For the square-to-2–R oval groove rolling test, square specimens with 52 mm sides and 300 mm length were machined. Fig. 4 shows the roll groove shape designed for the rolling test.

### *4.3 Test procedure*

The specimens were soaked in a reheating furnace at 1100 °C for 40 min to ensure homogenous temperature distribution. Before rolling, the surface temperature was measured at each pass using a high temperature pyrometer. The square specimen was first rolled into the 2–R oval groove [Fig. 4(a)], and then the rolled specimen was air-cooled to room temperature. For the round-to-2–R oval groove rolling, the specimen with the round section was first rolled into the 2–R oval groove [Fig. 4(b)], and then rolled into the round groove [Fig. 4(c)] after being rotated by 90° about the lengthwise direction. Entry guides were installed in front of each roll groove to minimize lateral bending of the specimen.

After the experiment, we obtained 10 mm-thick cross-sections by cutting the middle part of the workpiece along the lengthwise direction. Finally, the coordinates of the surface profile and the cross-sectional area were obtained using a surface profile reading program, followed by scanning the cross-section of the workpiece.

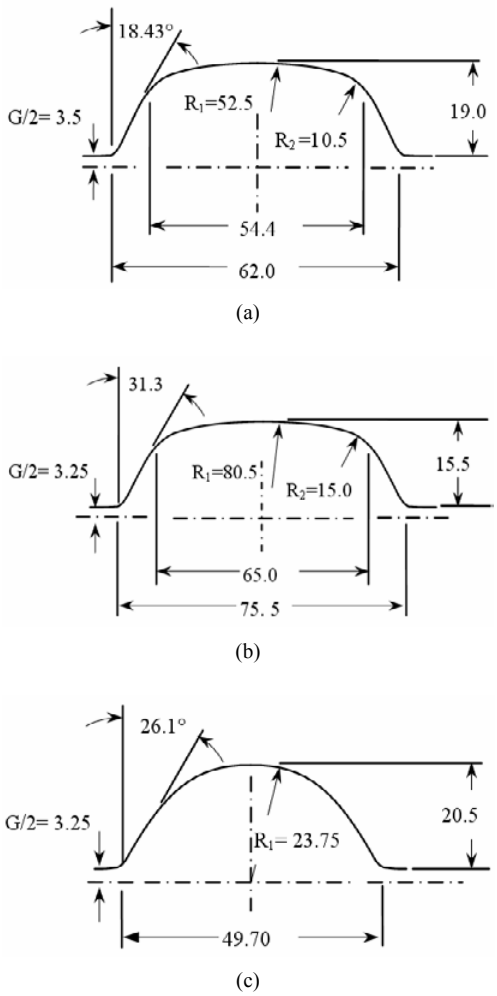


Fig. 4. Design parameters and roll groove used in groove rolling test. 2−R oval groove (A) (b) 2−R oval groove (B) and (c) round groove.

## 5. Results and discussion

Figs. 5-7 shows the comparison of the predicted surface profiles and the measured profiles for the square section-to-2–R oval, round-to-2–R oval, and 2–R oval-to-round groove rolling sequences. Note that the section height, represented as "SH," varies to some extent beyond the design roll gap (groove height) in each rolling test. The dash-dot line represents the roll groove shape, the dotted line indicates the measurements, and the solid line indicates the model predictions.

### *5.1 Square-to-2-R oval groove rolling*

Fig. 5(a) shows the results of square-to-2–R oval groove rolling when low carbon steel (S10C) was rolled.

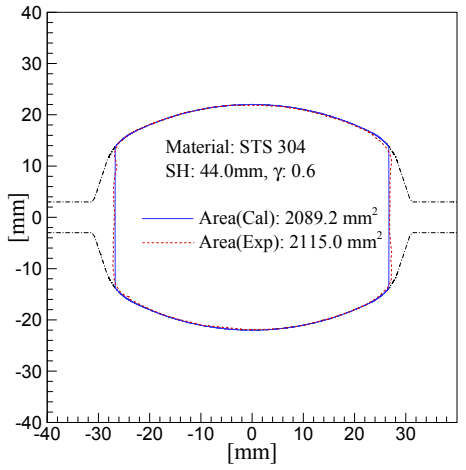


(a)

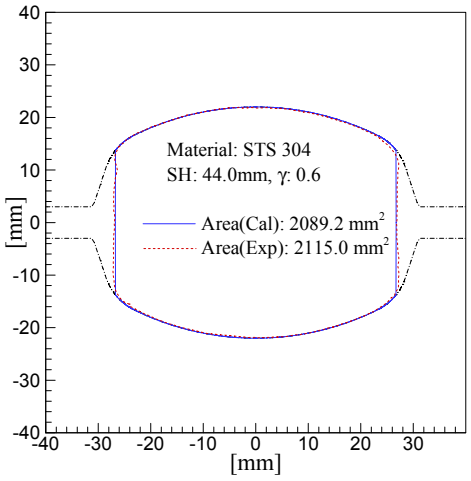


(b)

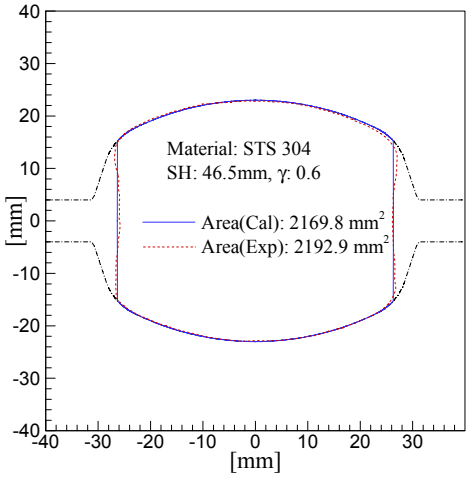


(c)

Fig. 5. Predicted and measured surface profiles of the exit cross-section for square section-to-2−R oval groove rolling. "γ" stands for a spread correction coefficient dependent on the material and type of rolling sequence. "SH" denotes the height of a roll groove.

Fig. 5(b) compares the measured surface profile with the predicted profile for stainless steel. For both cases, the measured cross-sectional area and the surface profile slightly exceeds the predicted values. Parameter γ indicates that the spread correction coefficient is dependent on the material and the type of rolling sequence. The spread correction coefficient was set to 0.45 for low carbon steel rolling and 0.6 for stainless steel rolling. The measured surface temperatures right before rolling was 1048°C for low carbon steel and 1104°C for stainless steel.

Almost no difference between the measured cross-sectional area shown in Fig. 5(a) and the area shown in Fig. 5(b) is observed, even though the SH of the 2−R oval groove in Fig. 5(b) was 1 mm larger than the height shown in Fig. 5(a). This is because 50 mm × 50 mm square specimens were rolled instead of 52 mm × 52 mm. The thermal expansion coefficient is 11.0 E-6/K for low carbon steel (0.1% C) and 17.3 E-6/K for stainless steel (STS304). The fit between the stainless steel specimen and the entry guide in front of the groove was so tight that the stainless steel specimen could not be positioned inside the entry guide. Hence, the specimen's dimensions had to be reduced. Thus, the 52 mm × 52 mm square specimen was reduced to a 50 mm × 50 mm for stainless steel rolling. Fig. 5(a) and (b) directly demonstrates the effect of the thermal expansion coefficient on the spread of the workpiece and consequently, its exit cross-sectional area in the hot rod rolling process.

The surface profile following the square-to-2−R oval groove rolling is not always a straight line; it can curve inward or bulge outward, depending on the reduction ratio. Fig. 5(c) shows the effect of the reduction ratio on the surface profile. The measured surface profile is slightly curved inward due to a relatively a low reduction ratio of 13.5% (see right-hand side of workpiece surface profile). Compressive forces caused by the upper and lower roll grooves are not strong enough to stretch the material in the roll gap direction. However, a higher reduction ratio does not always ensure that the outgoing surface profile of the workpiece will bulge outward, as is shown in Fig. 5(a) for the relatively high reduction ratio of 22.5%. If the reduction ratio increases significantly (about 30%), the surface profile of the workpiece might bulge outward. However, this cannot occur as the square specimen cannot be bitten in the 2−R oval groove because of the geometric constraint between the specimen cross-section and the 2−R groove section.

### *5.2 Round-to-2−R oval groove and 2−R oval-to-round groove rolling*

A comparison between the predicted surface profile and the measured profile was made when a specimen with a round section was rolled in the 2−R oval groove (Fig. 6). The predicted cross sectional area is generally in good agreement with the measured area for both passes. Spread correction coefficient γ is 0.95 for stainless steel and 0.85 for low carbon steel.

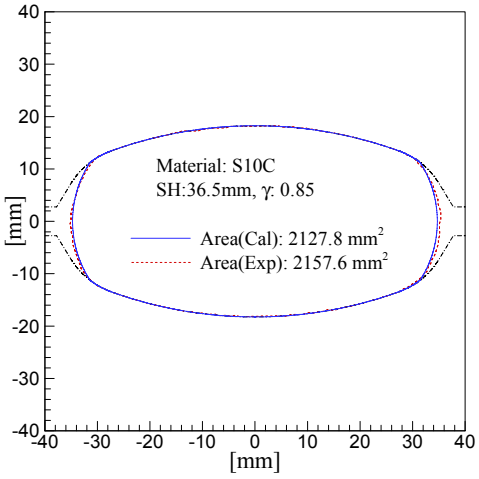


(a)

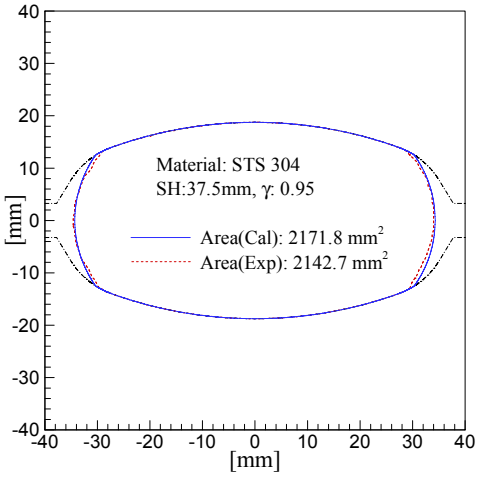


(b)

Fig. 6. Predicted and measured surface profiles of the exit cross-section for a round section-to-2−R oval groove rolling. "γ" stands for the spread correction coefficient dependent on the material and type of rolling sequence. "SH" denotes the height of a roll groove.

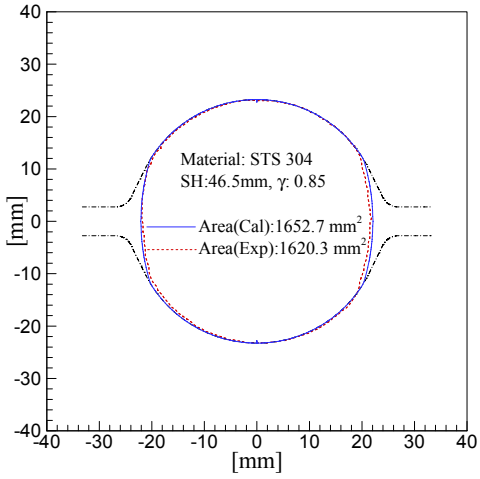


(a)

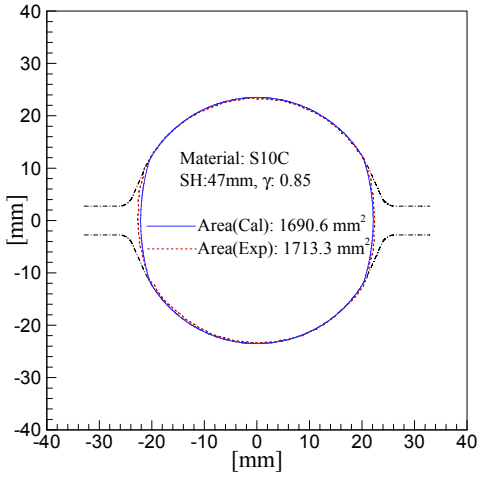


(b)

Fig. 7. Predicted and measured surface profiles of the exit cross-section for 2−R oval section-to-round groove rolling. "γ" stands for the spread correction coefficient dependent on the material and type of rolling sequence. "SH" denotes the height of a roll groove.

The surface profiles for both steels are similar. The higher spread correction coefficient (γ=0.95) may be attributed to the higher thermal expansion coefficient of stainless steel and the geometry of the 2−R oval groove. When a round specimen of 60 mm diameter was rolled in the 1−R oval groove rolling, a value of γ=0.83 was used [9]. This slight increase in the spread correction coefficient can be explained as follows. The second radius of curvature of the 2−R oval groove reduces the exit cross-sectional area of the workpiece, but helps squeeze the workpiece outward (i.e., in the roll gap direction) in the course of rolling because the radius of the stress-free surface profile of the outgoing workpiece in the 2−R oval groove is smaller than that in the 1−R oval groove.

Fig. 7 shows that the workpiece rolled out of the 2–R oval groove was rolled in the round groove. Careful comparison of the oval groove profile to the measured exit cross-sectional shape of the workpiece illustrates that the lower roll is slightly unbalanced along the lengthwise direction during rolling. Overall, the differences between the measured pass area (i.e., the exit cross-sectional area) and the predicted area are in the range of -1.3%–2.0%. The results obtained demonstrate that the analytical model proposed in this study has an experimental rationale for use in an actual rod mill where 2−R oval-to-round (or vise versa) groove rolling sequences are employed.

## 6. Concluding remarks

An analytical model that predicts the surface profile of a workpiece in 2−R oval-to-round (or vice versa) groove and square-to-2−R oval groove rolling was proposed. The effectiveness and generality of the model was analyzed after a series of pilot groove rolling tests with low carbon steel and stainless steel.

The proposed model can compute the surface profile of the

workpiece very quickly (in a second) if the inlet cross-section of the workpiece, the geometry of the roll groove, and a proper spread correction coefficient are known. The correction coefficient for the 2–R oval-to-round (or vice versa) groove is slightly higher than that of the 1–R oval-to-round (or vice versa) groove. The proposed model can serve as a highly valuable tool because it saves computational time. The finite element method requires considerable computation in predicting the surface profile of the workpiece in groove rolling.

## Acknowledgment

This research was supported by the Chung-Ang University Research Scholarship Grants in 2008.

## References

[1] S. M. Byon and Y. Lee, Experimental study for roll gap adjustment due to roll wear in single - Stand rolling and multi-stand rolling test, *Journal of Mechanical Science and Technology*, 22 (2008) 937-945.

[2] J. J. Park and S. I. Oh, Application of three dimensional finite element analysis to shape rolling process, *Journal of Engineering Industry*, 112 (1990) 36-46.

[3] N. Kim, S. M. Lee, W. Shin and R. Shivpuri, Simulation of square-to-oval single pass rolling using a computationally effective finite-slab element method, *Journal of Engineering Industry*, 114 (1992) 329-335.

[4] S.-Y. Kim and Y.-T. Im, Three-dimensional finite element analysis of non-isothermal shape rolling, *Journal of Materials Processing Technology*, 127 (2002) 57-63.

[5] S. Y. Kim, H. W. Lee, J. H. Min and Y. T. Im, Steady-state finite element simulation of bar rolling processes based on rigid-viscoplastic approach, *International Journal for Numerical Methods in Engineering*, 63 (2005) 1583-1603.

[6] H. J. Kim, T. H. Kim and S. M. Hwang, A new free surface scheme for analysis of plastic deformation in shape rolling, *Journal of Materials Processing Technology*, 104 (2000) 81-93.

[7] Y. Lee and S. Choi, New approach for the prediction of stress free surface profile of work piece in rod rolling, *ISIJ International*, 40 (2000) 624-626.

[8] Y. Lee, Prediction of the surface profile and area of the exit cross section of workpiece in round-oval-round pass sequence, *ISIJ International*, 42 (2002) 726-735.

[9] Y. Lee, Rod and bar rolling: theory and applications, *Marcel and Dekker Inc.*, New York, USA (2004).

[10] T. Shinokura and K. Takai, A new method for calculating spread in rod rolling, *Journal of Applied Metalworking*, 2 (1983) 175-188.

**U. K. Yoo** received his bachelor's degree in 2008 and Master's degree in 2010 in Mechanical Engineering from Chung-Ang University. His research area is mainly the shape rolling. He is currently working at Fastener Engineering Team of GM Daewoo Auto & Technology.

**Youngseog Lee** received the B.S. in Mechanical Engineering from Pusan National University, Korea, in 1989. He then received the M.S. and Ph.D. degrees from Case Western Reserve University, Cleveland, Ohio, USA, in 1992 and 1997, respectively. Until 2003, he worked as a researcher at POSCO Technical Research Laboratories, Pohang, Korea. He is currently an Associate Professor in the Department of Mechanical Engineering, Chung-Ang University, Seoul, Korea. He is interested in computational fracture mechanics and analysis of rolling process.